

Simulation of heat and mass transfer in a multi-effect distillation plant for seawater desalination

Henning Raach*, Jovan Mitrovic

*Institute of Energy and Process Engineering, Thermal Process Engineering, University of Paderborn,
D-33095 Paderborn, Germany*

Tel. +49 (5251) 60-2403, Fax: +49 (5251) 60-3207; email: raach@vt.upb.de

Received 20 March 2006; Accepted 1 April 2006

Abstract

In the European project EasyMED an innovative, multi-effect distillation plant for seawater desalination has been developed. The basic elements of each effect are vertical plates. On one side of a plate, seawater is distributed as a falling film, whereas on the other side, the plate is heated by condensing vapour generated in the previous effect. Our Institute is concerned with the heat and mass transfer in a system based on numerical experiments. Good agreement was achieved between a one-dimensional (1D) and a two-dimensional (2D) model capturing the evaporating falling film. Being less computationally expensive and sufficient for practical requirements, a 1D model was adopted for conjugate heat transfer between condensing and evaporating cells.

Keywords: Falling seawater film; Condensation; Evaporation; Conjugate heat transfer; Mass transfer; Nusselt

1. Introduction

In the European project EasyMED [1], an innovative, multi-effect distillation plant for seawater desalination has been developed. Involved

are partners from France, Italy, and Germany. The objective was to develop a prototype plant which is easy to operate and which makes efficient use of energy.

The basic elements of each effect are vertical plates. On one side of a plate, seawater is distributed as a falling film, whereas on the other side,

*Corresponding author.

Presented at the EuroMed 2006 conference on Desalination Strategies in South Mediterranean Countries: Cooperation between Mediterranean Countries of Europe and the Southern Rim of the Mediterranean. Sponsored by the European Desalination Society and the University of Montpellier II, Montpellier, France, 21–25 May 2006.

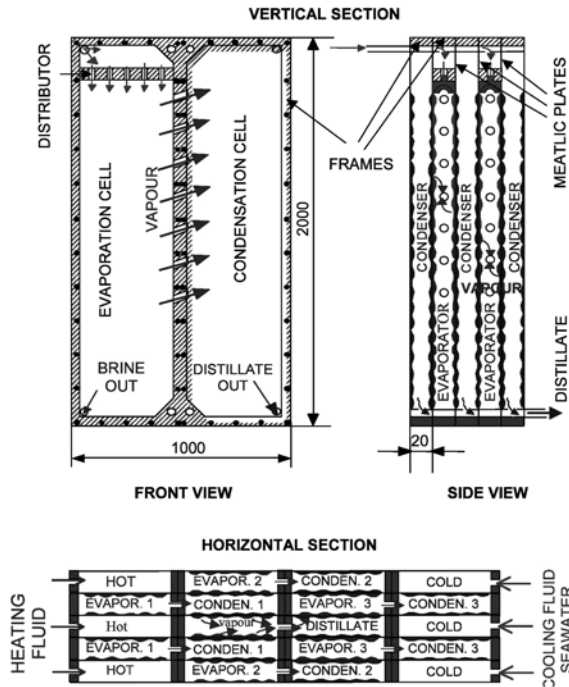


Fig. 1. Cross-sectional views of the EasyMED desalination unit as provided by our French partner from Nancy.

the plate is heated by condensing vapour generated in the previous effect (Fig. 1). In the evaporating cell, the seawater film immerses horizontal wires. On the one hand, these wires homogenise the film, preventing it from breaking up and leaving dry patches on the heating plate. On the other hand, they promote turbulence also at lower Reynolds numbers, thus augmenting the heat transfer across the falling film. This is the reason why they are called turbulence wires.

Our Institute is concerned with the heat and mass transfer in the system based on numerical experiments. In a previous publication [2], much of our results obtained in the project were summarised. This publication deals mainly with the improvement of the heat transfer by means of the turbulence wires. A 1D model was formulated that ignores the wires but captures the heat and mass transfer of the entire film. In the present

work, the 1D model is further developed and compared to a 2D model. As will be shown, the 1D description of the system is sufficient for practical needs. Therefore, a 1D program has been written that treats simultaneously vapour condensation and falling film evaporation, mass transport inside the saltwater film, and conjugate heat transfer through the conducting metallic plate.

2. Nusselt’s water–skin theory

For thin liquid films, evaporating as well as condensing, there is already a theory [3], which shall be briefly outlined here. Further improvements that are possible with the aid of computers are pointed out below.

For an evaporating film, Nusselt’s theory gives a parabolic velocity profile

$$v = \frac{g \cdot \delta^2}{\nu} \left[\frac{x}{\delta} - \frac{1}{2} \left(\frac{x}{\delta} \right)^2 \right] \quad (1)$$

and a linear temperature distribution

$$T = T_w - (T_w - T_I) \frac{x}{\delta} \quad (2)$$

where x denotes the distance from the heating plate; T_w is the wall temperature; and T_I the saturation temperature of the vapour, which is assumed to be equal to the temperature of the liquid–gas interface (Fig. 2). Then the film thickness δ at distance y from the inlet is given by

$$\delta(y) = \left[\delta_{IN}^4 - 4 \frac{\lambda \nu (T_w - T_I)}{\rho \cdot g \cdot \Delta h} \right]^{1/4} \quad (3)$$

where δ_{IN} denotes the initial (inlet) film thickness, Δh the evaporation enthalpy, λ the thermal conductivity, and ρ the density of the liquid phase.

For a condensing film, the velocity profile obeys Eq. (1). The temperature distribution

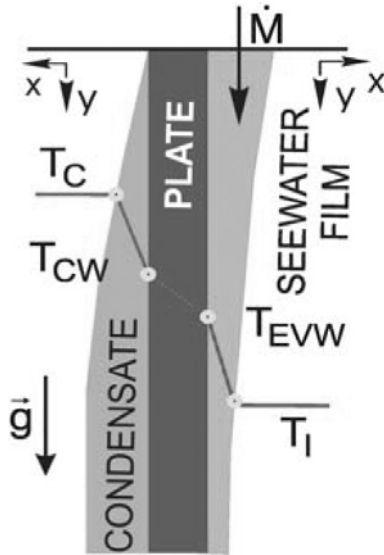


Fig. 2. Physical model.

between the cooling wall and the vapour at saturation temperature is still linear, and Eq. (2) is appropriate. In this case, however, T_i is greater than T_w , and the second term in brackets changes sign. Also Eq. (3) is valid in the case of film condensation. Again the temperature difference changes sign and there is an increase of the thickness farther downstream. Note that the derivation of this equation rests on the assumption that a constant driving temperature difference, disregarding at the same time the energy change of the film due to heating or cooling. For details concerning these effects, refer to the literature, e.g., Mitrovic [4].

3. Models of evaporating saltwater film

3.1. One-dimensional model

A 1D model of an evaporating seawater film that is heated by a plate of constant temperature was described earlier [2]. Only a major change is noted here. As the film is heated, its properties change, namely the density and kinematic viscosity. Assuming a Nusselt velocity profile,

Eq. (1), the mass flow rate is

$$\dot{M} = \frac{\rho}{3\nu} \cdot g \cdot b \cdot \delta^3 \quad (4)$$

where g is the gravitational acceleration, b the width of the film (plate), and δ the film thickness. As follows from Eq. (3), the change of the film thickness δ along the flow direction y depends on the physical properties and the driving temperature difference, $T_w - T_i$. Neglecting, for the moment, the evaporation effect, that is to say, omitting the second term in brackets of Eq. (3), Eq. (4) gives

$$\delta = \left(\frac{\rho_{IN}}{\rho} \frac{v}{v_{IN}} \right)^{1/3} \delta_{IN} \quad (5)$$

where v and ρ are the average properties in the cross-sectional flow area of the film at distance y . We have replaced δ_{IN} in Eq. (5) by $\delta(y)$ according to Eq. (3) and used it in the present model.

3.2. Two-dimensional model

In order to check the 1D model, a more realistic 2D description of the system was formulated and implemented in a computer program which includes the heat and mass transfer by diffusion and convection according to the expression

$$\frac{\partial(\rho\Phi)}{\partial t} + \frac{\partial(\rho\Phi v)}{\partial y} = \text{div}(\Gamma_\Phi \text{grad } \Phi) + R_\Phi \quad (6)$$

In our case, the scalar Φ is the temperature T or salinity S . The second term on the left-hand side of Eq. (6) is the convective part corresponding to velocity v in the y direction. The first term on the right-hand side is the diffusion term containing the coefficient Γ_Φ . To solve for the temperature, $\Gamma_T = \lambda c_p$, where c_p is the specific heat. If salinity S is to be determined, $\Gamma_S = D\rho$, where D is the

salt diffusivity. The term R_{ϕ} denotes numerical sources that usually appear when a certain boundary condition is to be imposed (e.g., a constant wall temperature).

For the solution of Eq. (6), the finite volume method is employed with a fully implicit scheme for temporal changes and central differences for the spatial derivatives [5,6]. An adaptive mesh is used, which means that the number of cells in the x direction is kept constant, while the film thickness δ and thus the cell size Δx changes due to evaporation. During a time step Δt , the film thickness δ is reduced by $\Delta_e \delta$ according to

$$\Delta_e \delta = \frac{\lambda \left| \frac{\partial T}{\partial x} \right|_I}{2\rho \cdot \Delta h} \cdot \Delta t \quad (7)$$

Also the convective change must be taken into account; thus,

$$\Delta \delta = -v \cdot \left(\frac{\partial \delta}{\partial y} \right) \cdot \Delta t - \Delta_e \delta \quad (8)$$

The velocity is calculated according to the Nusselt formula, Eq. (1), and it depends on the fluid properties and the film thickness.

On the film surface, water evaporates, leaving the salt in the remaining seawater film. This leads to an increase of the salinity in the cell next to the interface:

$$\Delta S = S_{IN} \cdot \left(\frac{\Delta_e \delta}{\Delta x_{IN}} \right) \quad (9)$$

In Eq. (9), S_{IN} denotes the initial salinity, $\Delta_e \delta$ the change of the film thickness by evaporation [Eq. (7)], and Δx_{IN} the initial cell size in the x direction. As the amount of salt in the film does not change, the conservation integral

$$\int_0^{\delta} S \, dx = \text{const} \quad (10)$$

is required to hold.

3.3. Comparison of 1D and 2D models

A comparison was performed between the 1D and 2D model that both describe a falling evaporating seawater film heated by a vertical plate. The wall temperature was kept constant at $T_w = 65^\circ\text{C}$ and the seawater inlet temperature and the salinity were at $T_{IN} = 60^\circ\text{C}$ and $S_{IN} = 35 \text{ g/kg}$, respectively. The temperature difference of 5°C relates to the temperature decrease between neighbouring effects in the EasyMED desalination plant. The Reynolds number Re is defined by

$$Re = \frac{\dot{M}}{b \cdot \mu} = \frac{\rho \cdot \delta \cdot \bar{v}}{\mu} \quad (11)$$

where \dot{M} denotes the mass flow rate, b the plate width, μ the viscosity, ρ the density and \bar{v} the average velocity, was varied.

Table 1 shows a comparison of the models for selected Reynolds numbers. The flow rates corresponding to Re in the case of the EasyMED desalination plant are also displayed. The first comparison deals with the decrease of the film thickness at the bottom of the 1.5 m long plate. The reduction of the film thickness is measured in terms of the initial film thickness. The second and third comparison criteria are the salinity at the interface S_{ENDI} and the temperature of the interface T_{ENDI} , both determined at the bottom of the plate, the index I referring to the interface. As the interface salinity depends on the number of cells in the x direction, this number was the same in the 1D and 2D program. The interface temperature is higher than 60°C because the average salinity in the film increased due to evaporation. It was observed in the numerical experiments that, after a short entrance region of approximately 10 cm, the temperature profiles of the 1D and 2D programs were both linear [Eq. (2)].

It can be seen from Table 1 that the agreement of the 1D and 2D models is good. Considering that calculations with the 2D program take

Table 1
Comparison between 1D and 2D programs, $S_{IN} = 35$ g/kg

Flow rate, l/h	Re	$\Delta\delta_{END}/\delta_{IN}$, %		S_{END} , g/kg		T_{END} , °C	
		1D	2D	1D	2D	1D	2D
25	37	53.7	60.3	92.44	108.4	61.55	62.11
50	73	13.3	12.5	52.66	53.76	60.17	60.14
100	147	5.3	4.4	43.62	44.09	60.06	60.05
150	220	3.5	2.5	41.77	41.19	60.04	60.03

several days, whereas the results with the 1D model are obtained in several minutes, the 1D program should be preferred.

4. Conjugate heat transfer

4.1. Method

For the reasons stated above, we adopted the 1D program for simulating the conjugate heat transfer between the condensing water film on the one side of the plate and the evaporating seawater film on the other side. In this program an adaptive grid was used, i.e., the number of cells was constant whereas their coordinates varied according to the changing film thicknesses. The film thickness of the evaporating saltwater film is calculated by

$$\delta(y) = \left[\delta_{IN}^4 - \int_0^y 4 \frac{\lambda_v (T_W - T_I)}{\rho \cdot g \cdot \Delta h} dy \right]^{1/4} \quad (12)$$

Note that the above relation is more accurate than Eq. (3) of the Nusselt theory since all quantities in the integral kernel can be treated as functions of the distance from inlet y . For the condensing water film, the same equation is used. In this case, the variables in Eq. (12) may have other values for the temperatures on the other side of the plate and the initial film thickness are different and the condensate film does not contain any salt.

To calculate the salinity in the seawater film, again Eqs. (9) and (10) are employed and a 1D diffusion equation is solved in the domain of the saltwater film. The energy equation is simultaneously solved for in the condensing film in the plate and in the saltwater film. The surface temperature of the condensing film is assumed to be equal to the constant vapour temperature. The surface temperature of the saltwater film is the saturation temperature which basically may change along the film flow because of the salinity increase due to evaporation. The simulation is transient. The elapsed time is worked out in the distance from the inlet y according to the velocity at the interface of the evaporating film.

4.2. Representative results

Numerical experiments were performed with a temperature of heating, condensing vapour of 65°C and an initial temperature of 60°C for the seawater film and the plate. Again, a temperature difference of 5°C is assumed as in Section 3. However, the simulation is now more realistic since the temperature drop in the condensate film and inside the plate is determined and the wall temperatures are no longer constant. The initial salinity was 35 g/kg. An initial thickness of the condensing film of 0.05 mm was chosen. The stainless steel plate was 1 mm thick.

As an example, Fig. 3 shows the temperature distribution along the falling film at a Reynolds

Table 2
Results from 1D simulation of conjugate heat transfer

Evaporating film				Wall temperatures		Heat flux
Flow rate, l/h	Re	$\Delta\delta_{END}/\delta_{IN}$, %	T_{END} , °C	T_{EV} , °C	T_{CON} , °C	q_{END} , kW/m ²
25	37	16.5	60.2	62.31	63.09	11.5
50	73	6.7	60.07	62.68	63.36	10
100	147	3	60.03	63	63.59	8.6
150	220	2	60.02	63.14	63.68	8

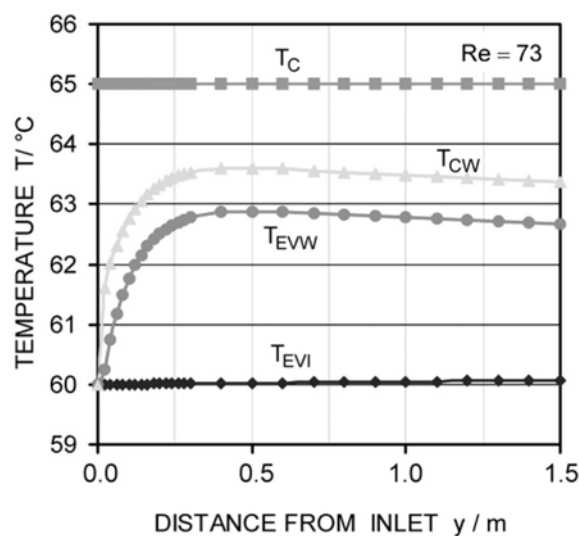


Fig. 3. Temperatures at the boundaries of the two films in dependence of distance from the inlet.

number of 73. The temperature of the vapour, the temperature of the wall on the condensation side and on the evaporation side, and the interface temperature of the saltwater film are displayed. These profiles correspond to the heat flux q that is at the inlet zero in the plate and in the seawater film but (for numerical purposes) 65 in the condensing film. When the heat flux approaches a common value in the three parts of the system, the temperatures in Fig. 2 have an approximately constant value. The wall temperatures then undergo a slight decrease along the plate because the film thicknesses change due to condensation on one side and evaporation on the other side.

Table 2 summarises the results. It shows the relative decrease of the seawater film thickness, the surface temperature of the evaporating film, the wall temperatures and the heat flux. The values listed in Table 2 all refer to the bottom of the plate, which has a height of 1.5 m. A comparison to the data in Table 1 reveals that the evaporation is weaker now. This is due to a lower wall temperature, which arises from the temperature drop in the condensate film and inside the plate.

5. Conclusions

An evaporating seawater film running down a vertical plate of constant temperature was simulated with a 1D and a 2D program. Because of good agreement of both models, the 1D description was considered as sufficient for practical purposes. Being at the same time considerably more efficient, a 1D program was written that captures the conjugate heat transfer between the condensing film, plate, and evaporating saltwater film, allowing for the surface temperature of the plate to adjust itself according to the heat and mass transfer conditions in the films falling across the plate.

The main result of our numerical simulations is the change of the plate temperature along the film flow. Because of the specified inlet conditions, the temperature of the plate first increases downstream, reaching a maximum that is followed by a temperature decrease. The decrease of

the plate temperature is rooted in the corresponding changes of the heat transfer resistances in the films due to vapour condensation and film evaporation.

All three programs developed within the EasyMED project are available on the internet [6].

6. Symbols

b	—	Width of plate
D	—	Diffusion coefficient
g	—	Acceleration due to gravity
Δh	—	Enthalpy of phase change
M	—	Mass flow rate
R	—	Source
S	—	Seawater salinity
T	—	Temperature
t	—	Time
v	—	Velocity in y direction
\bar{v}	—	Average of v
x	—	Orthogonal coordinate
y	—	Vertical coordinate

Greek

δ	—	Film thickness
λ	—	Thermal conductivity
μ	—	Dynamic viscosity
ν	—	Kinematic viscosity
ρ	—	Density
Φ	—	Dummy variable
Γ	—	Dummy parameter

Subscripts

END	—	At plate bottom
EV	—	Evaporation
C	—	Condensation
I	—	Film interface
IN	—	At inlet, plate top
W	—	Wall, plate surface

Acknowledgements

The EasyMED project was financed by the European Union. The authors would also like to acknowledge the friendly cooperation with the partners.

References

- [1] www.easymed-eu.com.
- [2] H. Raach and J. Mitrovic, Seawater falling film evaporation on vertical plates with turbulence wires, *Desalination*, 183 (2005) 307–316.
- [3] W. Nusselt, Die Oberflächenkondensation des Wasserdampfes, *Zeitschrift VDI* 60, No. 27, 1916, pp. 541–546.
- [4] J. Mitrovic, The Nusselt condensation and nonisothermality, *Int. J. Heat Mass Transfer*, 41 (1998) 4055–4061.
- [5] H.K. Versteeg and W. Malalasekera, *An Introduction to Computational Fluid Dynamics — The Finite Volume Method*, Pearson-Prentice Hall, New York, 1995.
- [6] J.H. Ferziger and M. Peric, *Computational Methods for Fluid Dynamics*, 3rd ed., Springer, 2002.
- [7] www.tvt.upb.de/~raach/easymed.html.